Published in final edited form as:
Environ Sci Technol. 2012 June 5; 46(11): 5834–5841. doi:10.1021/es300603s.

Geochemical Weathering Increases Lead Bioaccessibility in Semi-Arid Mine Tailings

Sarah M. Hayes[1], **Sam M. Webb**[2], **John R. Bargar**[2], **Peggy A. O'Day**[3], **Raina M. Maier**[1], and **Jon Chorover**[1,*]

[1]Department of Soil, Water and Environmental Science, University of Arizona, Tucson, AZ 85721

[2]Stanford Synchrotron Radiation Laboratory, SLAC National Accelerator Laboratory, 2575 Sand Hill Road, MS 69, Menlo Park, California 94025

[3]School of Natural Sciences, University of California, Merced, CA 95343, USA

Abstract

Mine tailings can host elevated concentrations of toxic metal(loid)s that represent a significant hazard to surrounding communities and ecosystems. Eolian transport, capable of translocating small (micrometer-sized) particles, can be the dominant mechanism of toxic metal dispersion in arid or semi-arid landscapes. Human exposure to metals can then occur via direct inhalation or ingestion of particulates. The fact that measured doses of total lead (Pb) in geomedia correlate poorly with blood Pb levels highlights a need to better resolve the precise distribution of molecularly-speciated metal-bearing phases in the complex particle mixtures. Species distribution controls bioaccessibility, thereby directly impacting health risk. This study seeks to correlate Pb-containing particle size and mineral composition with lability and bioaccessibility in mine tailings subjected to weathering in a semi-arid environment. We employed X-ray absorption spectroscopy (XAS) and X-ray fluorescence (XRF), coupled with sequential chemical extractions, to study Pb speciation in tailings from the semi-arid Arizona Klondyke State Superfund Site. Representative samples ranging in pH from 2.6 to 5.4 were selected for in-depth study of Pb solid-phase speciation. The principle lead-bearing phase was plumbojarosite ($PbFe_6(SO_4)_4(OH)_{12}$), but anglesite ($PbSO_4$) and iron oxide-sorbed Pb were also observed. Anglesite, the most bioavailable mineral species of lead identified in this study, was enriched in surficial tailings samples, where Pb concentrations in the clay size fraction were 2–3 times higher by mass relative to bulk. A mobile and bioaccessible Pb phase accumulates in surficial tailings, with a corresponding increase in risk of human exposure to atmospheric particles.

Keywords

XAS; sequential extraction; semi-arid mine tailings; lead speciation; anglesite

1. INTRODUCTION

The human health impacts of mine tailings have come under increasing scrutiny in recent decades. Most research and remediation efforts have focused on temperate climates where high precipitation results in formation of acid mine drainage (AMD). However, recent

*Address correspondence to Jon Chorover, Department of Soil, Water and Environmental Science, University of Arizona, 1177 E 4th St, Shantz 429, Tucson, AZ 85721 Telephone: 520-626-5635, Fax: 520-626-1647, chorover@cals.arizona.edu.

7. SUPPORTING INFORMATION AVAILABLE Text, tables, and figures describing sample preparation, characterization, and spectroscopic analysis. This information is available free of charge via the Internet at http://pubs.acs.org.

studies of mine tailings in arid climates, where a large proportion of exposed, uncapped tailings piles exist, have revealed the importance of human exposure to metal-containing tailings particles dispersed by wind.[1–3] Atmospheric transport over local to regional and even global distances disperses small (i.e., ≤ 35 μm) particulate mineral-weathering products formed in mine tailings systems. Particles smaller than 10 μm pose an inhalation health risk, whereas risk of exposure via ingestion extends to larger particle sizes.[4–6] Highest aerosol exposures are expected in communities that exist downwind in close proximity to tailings piles, whereas a logarithmic decay of particle concentrations is expected further down-gradient.[7]

Lead (Pb) is among the geo-dust metals of greatest concern because of its prevalence in exposed sulfide ore deposits and its known pediatric neurological impacts even at low concentration.[4] The CDC regulatory limit for blood Pb is 10 μg dL^{-1},[8] but a statistical reduction of IQ has been reported even in children with blood Pb levels of 10 μg dL^{-1} compared to those with1 μg dL^{-1}.[9] Several studies have reported weak correlations between total Pb exposure and blood Pb levels in mining-impacted communities,[10] supporting the concept that Pb speciation controls its bioavailability, and that total Pb exposure is an insufficient predictor of health effects.

Several studies have examined Pb bioavailability via feeding experiments and efforts have been made to correlate these observations with *in vitro* extractions. One such study, using a swine ingestion model to predict child uptake and relative bioavailability of Pb in 19 mining-impacted soils, slag, and tailings, concluded that plumbojarosite and anglesite have low and medium bioavailability, respectively, relative to high-bioavailability soluble lead acetate.[11] A rabbit model study indicated that 10% of Pb in anglesite-dominated mine tailings dissolved in the stomach and was available for absorption in the intestine.[12] *In vitro* simulation of stomach conditions indicated that a maximum of 4% of Pb from ingested mine tailings was solubilized during gastrointestinal residence time, pointing to kinetic limitations on toxicity.[13] Despite criticisms regarding dissolution of nontarget phases and artifacts,[14–16] sequential extractions (SE) remain a useful quantitative metric of Pb lability[17]. For example, by combining SE and bioaccessibility extractions, bioaccessible Pb in mine tailings has been well correlated to the mass extracted in water plus ammonium oxalate solutions.[3] Likewise, a feeding study showed that bioavailability of soil Pb could be predicted from that solubilized during SE steps targeting water soluble, exchangeable, carbonate, weak organic complexes, and Mn-oxide associated Pb.[18] Both feeding and *in vitro* studies have reported a variety of bioaccessible Pb forms in contaminated geomedia, highlighting the importance of Pb speciation, mineralogy, and particle size.[18–24] However, direct evidence relating the bioavailable fraction(s) to quantitative chemical extraction and Pb bonding environment is needed for tailings weathered in arid environments; exposure risks for uncapped and unvegetated desert tailings are high, and the link between Pb speciation and bioavailability is clear.

Because of lead's potential toxicity, its geochemical transformations in mine wastes have been studied extensively.[3, 25–27] Galena (PbS) is often deposited with variable amounts of accessory silicate and carbonate gangue minerals. Geochemical weathering under oxic conditions results in the formation of various secondary products including cerrusite ($PbCO_3$), anglesite ($PbSO_4$), and plumbojarosite ($PbFe_6(SO_4)_4(OH)_{12}$), each of which has distinct bioaccessibility.[28] Lead also occurs as a sorbed species, often associated with jarosite ($KFe_3(SO_4)_2(OH)_6$), and Fe (oxyhydr)oxides.[29–31] We hypothesize that the low (< 50 cm) precipitation and high evapotranspiration rates that typify arid and semi-arid regions results in the persistence of soluble sulfate phases (such as efflorescent salts) formed, in part, by the upward migration of metal-rich pore waters driven by capillary action in uncapped

tailings.[17, 26, 32] However, detailed Pb molecular speciation is necessary to accurately assess the associated health risks, particularly to determine if bioavailable salts persist.

X-ray absorption spectroscopy (XAS) is one of the only methods capable of providing direct molecular-scale speciation of Pb in natural geomedia. Several studies have employed XAS to probe Pb speciation in mine tailings.[29, 33–35] Most of the tailings studied were carbonate rich, and Pb was principally found in carbonate and sorbed phases.[29, 35] The particular importance of sorbed species in mine and smelter impacted soils has been highlighted,[34] as has the prevalence of plumbojarosite, relative to such solids as plumboferrite ($Pb_2Fe_{11}O_{19-\delta}$), and vanadinite ($Pb_5(VO_4)_3Cl$).[29] Additionally, XAS has been used to examine the effects of digestion on the speciation of Pb in contaminated geomedia with one result being that Pb associated with Fe (oxyhydr)oxides, particularly ferrihydrite, contributes significantly to the bioaccessible Pb pool, possibly due to dissolution and reprecipitation during GI fluid extraction.[23, 36, 37]

The overall goal of the current project was to assess Pb speciation in the near-surface depths of uncapped mine tailings that have undergone weathering in a semi-arid desert environment. The Klondyke State Superfund Site is the subject of intense interest because it comprises mine tailings devoid of vegetation located at the mouth of Aravaipa canyon, an important riparian corridor in southeastern Arizona. The tailings pile exhibits a large range in pH (2.5– 8.0) that results from a semi-arid weathering trajectory toward increasingly acidic conditions.[17] Speciation of co-contaminant Zn was studied previously, and it was shown to favor highly mobile Zn forms under oxic weathering conditions, supported by an order of magnitude decrease in Zn concentration with progressive tailings acidification. During weathering, Zn released from sphalerite (ZnS) incorporates into secondary silicate clays (i.e., Zn-talc-like coordination), iron oxide-sorbed Zn species and, persistent zinc sulfate phases.[38] Given the high concentrations of Pb present in the tailings media, characterization of Pb speciation to better predict associated risks to surrounding communities and ecosystems is likewise warranted.

The specific objectives of the present study were, therefore, (i) to measure the distribution of Pb species in tailings samples at different depths (0–30 and 21–53 cm), (ii) to determine the fraction of bioavailable Pb in the tailings, and (iii) to assess the fraction of Pb that can be transported off site by wind dispersion. A chemical SE was combined with synchrotron-based bulk XAS and micro-focused X-ray fluorescence (XRF) and XAS to elucidate Pb speciation in the Klondyke tailings.

2. MATERIALS AND METHODS

2.1 Physical and chemical characterization

2.1.1 Reference materials—All reagents were ACS reagent grade or better and the identities of all spectroscopic crystalline reference materials were confirmed by X-ray diffraction analysis. A list of reference materials is located in the Supporting Information (SI).

2.1.2. Tailings collection—Tailing samples were collected from specific locations at the Klondyke State Superfund Site (ID# 1236) located in Graham County, Arizona. Additional site details and routine geochemical characterization of the tailings were reported previously in conjunction with a systematic tailings-wide sampling effort.[17] Based on those data, two surface samples (0–30 cm composites), $T^S_{5.4}$ and $T^s_{3.9}$, and two subsurface samples (28–53 cm and 21–42 cm composites), T^D $D_{4.2}$ and $T^D_{2.6}$ were selected for the present detailed study. In sample names, the superscripts denote surface (S) or subsurface (D) samples and subscripts denote tailings pH. After collection, tailings were sieved to obtain the fine earth

(< 2 mm) fraction, air dried for two weeks, and then stored at room temperature. In addition to tailings collected from the unvegetated field site, an efflorescent salt sample was collected from the top surface of planted tailings generated in a potted-plant growth trial that used $T_{3.9}$ as soil substrate. Samples were stored in sealed plastic bags prior to analysis. Initial analysis demonstrated that these samples contained high total concentrations of Pb (13.9, 4.4, 4.6, 4.7and 6.0 g kg^{-1} in $T^S_{5.4}$, $T^S_{3.9}$, $T^D_{4.2}$ $T^D_{2.6}$, and evaporite, respectively). Thin sections for each tailings sample were prepared by impregnation with EPOTEC 301-2FL epoxy under vacuum, and cured for three days before being sent to Spectrum Petrographics (Vancouver, WA), where they were sectioned to 30 μm, polished on both sides, and mounted on quartz slides.[17, 39]

2.1.3 Sequential chemical extraction—A six step SE method, developed for weathered sulfide mine tailings,[40] was used to quantitatively extract metals into operationally-defined fractions while targeting specific phases. The procedure[17] includes the following steps and target metal species: (i) "***H_2O***": water extraction of soluble salts; (ii) "***AA***": ammonium acetate extraction of exchangeable ions and calcite; (iii) "***AAO 25°C***": ammonium oxalate at 25°C extraction of short-range-order Fe, Al and Mn-(hydr)oxides and poorly-crystalline jarosite; (iv) "***AAO 80°C***": ammonium oxalate at 80°C extraction of crystalline Fe, Al, and Mn (hydr)oxides and jarosites; (v) "***H_2O_2***": hydrogen peroxide oxidative extraction of organic matter and secondary supergene sulfides; and (vi) "***Acid***": concentrated HCl and HNO_3 extraction of primary sulfides. The Zn content of the "***Residual***" was then determined by bulk X-ray fluorescence (see SI).

2.2 Lead concentration in size fractions

Particle size distributions of the < 2 mm size fractions were determined using a laser diffractometer (Beckman Coulter LS 13 320, Miami, Fl) in the UA Center for Environmental Physics and Mineralogy (Tucson, AZ). Isolation of sand, silt, and clay particle sizes was accomplished using the pipette sedimentation method.[41] Metal concentrations in the size-fractionated tailings were determined following microwave-assisted digestion of the tailings (US EPA Method 3051). Briefly, 0.1 g of ground tailings were suspended in 10 mL of concentrated nitric acid in Teflon vessels for 2 h before transferring the vessels to a CEM MDS-2100 microwave (Matthews, NC) for digestion during which the maximum pressure (15 psi) and temperature (154 °C) were monitored. After cooling, the digestate was transferred, and each vessel was rinsed with 15 mL of 18 MΩ water. The collected solutions (10 mL HNO_3 digestate and 15 mL rinse water) were filtered and diluted for elemental analysis by ICP-MS.

2.3 Bulk XAS collection

Lead speciation of the tailings samples and reference materials was investigated with Pb L_{III}-edge (E_0=13035eV) XAS spectroscopy. XAS spectra of the four tailings samples, the efflorescent salt, and the clay size (< 2.0 μm) fractions of $T^S_{3.9}$ and $T^S_{5.4}$ were collected at the Stanford Synchrotron Radiation Lightsource (SSRL, beam lines 10-2 and 11-2) or at GSE-CARS, beam line 13-BM, at the Advanced Photon Source (Argonne National Laboratory, IL) (see SI for details). A minimum of 3 scans were collected in transmission mode (used for most reference materials) and 10–15 scans were collected in fluorescence mode (used for tailings and sorption samples).

2.4 XAS data analysis

XAS spectra were analyzed using SIXPACK (version 0.63).[42] Energy was calibrated by collecting the absorption edge of a lead foil standard between every two samples, where the first maximum of the first derivative spectrum was defined as 13035 eV. Spectra were

averaged and then the adsorption edge and extended X-ray absorption fine structure (EXAFS) portions of the spectra were extracted for analysis. Backgrounds were subtracted using a linear fit to the pre-edge region (−210 to −100 or −50 eV below edge) that was extended through the spectrum. Spectral step heights were normalized using a quadratic post-edge (150 to ~570 eV for bulk and 50 to 150 eV for μ-XAS above edge). EXAFS oscillations were extracted using splines with low R-space reduction function (R_{bkg}), which minimizes the contribution from low frequency oscillations (i. e., peaks at low R), associated with physically impossible bond distances.[43] Of several tested, splines with R_{bkg}=1.5 and spline range 1 to 9 or 9.5 $Å^{-1}$, with no spline clamps, consistently gave the best fit statistics, as indicated by reduced χ^2 in shell-by-shell fits, for all samples and references, and thus were also used for subsequent analysis with linear combination fitting (see SI for details pertaining to linear combination fitting, and shell-by-shell fitting).

2.5 Micro-focused X-ray fluorescence mapping and X-ray absorption spectroscopy

Micro-focused XRF maps and XAS of samples in thin section were collected on beam line 2–3 at SSRL using a water-cooled double crystal monochromator with either a Si (220), ϕ=0 or Si (111) crystal and a vortex single element detector (SII Nano Technology, Northridge, CA). Elemental mapping was performed with a micro-focused beam (*ca.* 2.5 μm in cross-section) provided by a Pt-coated Kirkpatrick-Baez mirror pair (Xradia Inc.), in 2.5 μm steps and a 250 ms dwell time. A thin section was placed directly in front of the X-ray beam tuned to 13050 eV, just above the Pb L_{III} absorption edge. The XRF maps were analyzed using the Microanalysis Toolkit (version 0.47).[44] Each map was linearly scaled from lowest counts (black) to highest counts (white). The highest number of counts for Pb, Fe, and S were 5,000, 10,000, and 200, respectively. Micro-focused XAS data were collected over an extended XANES region (12800–13290 eV) using the same beam conditions as for the mapping.

3. RESULTS

3.1 Lead content, particle size and lability

Conjunctive particle size and total Pb analyses indicate that the clay-sized fraction (25–32% by mass) was 2- to 3-fold enriched in Pb relative to the bulk tailings (up to 50 g kg^{-1}; Fig. 1A and B). Results of the sequential extraction (Fig. 1C) indicate that Pb is mobilized significantly in the AA, H_2O_2, and acid steps. The AA step extracted a large mass of Pb from the surface samples (17–34%, Fig. 1C) that are also relatively enriched in fine particles (Fig. 1A,B) whereas the nitric acid step extracted a high proportion of total Pb mass from the most acidic, subsurface tailings. The sum of the first three SE fractions, representing the fraction of total Pb considered potentially bioaccessible, amounted to 38, 25, 11, and 3% in $T^S_{5.4}$, $T^S_{3.9}$, $T^D_{4.2}$, $T^D_{2.6}$, respectively.

3.2 Linear combination fits of lead XAS

Linear combination fits of the first-derivative XANES and EXAFS portions of the bulk XAS spectra (Fig. 2) were performed using plumbojarosite, anglesite and iron (oxhydr)oxide-sorbed Pb ($Pb_{ads\text{-}FeOx}$) references because they gave the best fit statistics and their presence was confirmed using other techniques including XRD and extraction to fit the tailings spectra. There is also qualitative agreement between the first derivative XANES and EXAFS fits indicating plumbojarosite is the principle lead-bearing phase in the Klondyke tailings. The fits also demonstrate anglesite enrichment in surficial tailings as indicated by the appearance of the shoulders at *k* values of 5.1 and 6.2 $Å^{-1}$. Bulk XRD analysis confirmed the presence of several sulfate salts in the evaporite sample, including, in order of estimated decreasing abundance: gypsum ($CaSO_4 \cdot 2H_2O$), anglesite, bianchite ($ZnSO_4 \cdot 6H_2O$), and jarosite (data not shown). Fit statistics indicate better fits for the tailings relative to the

evaporite, and the XANES fits are better than the EXAFS fits for all spectra (Table 1). EXAFS fit totals deviate from 100% by both overestimating (evaporate) and underestimating (tailings) the totals.

3.3 Shell by shell XAS analysis

Shell-by-shell analysis was used to confirm the presence of plumbojarosite in the tailings. The plumbojarosite reference and $T^{D}_{2.6}$, which was well-fit using only plumbojarosite, were both fit using three single scattering paths, developed from the crystal structure of plumbojarosite, at 2.69, 2.95, and 3.55 Å.[45] Bond distances consistent with the crystal structure of plumbojarosite – within 0.02Å for the first oxygen and within 0.06 Å for all other bond distances – were obtained for both the plumbojarosite reference and $T^{D}_{2.6}$, (Fig. 3 and Table 2). For $T^{D}_{2.6}$, the Debye-Waller factor - an indication of thermal and structural disorder - for the first shell (0.023 $Å^2$) was observed to be significantly higher than for the plumbojarosite reference (0.014 $Å^2$).

3.4 μ-XRF and μ-XAS

Micro-focused XRF images (Fig. 4A) show the elemental spatial distributions and identify Pb "hotspots" for XAS analysis. First- derivative XANES spectra (numbered in Fig. 4A) were fit to plumbojarosite, anglesite, and $Pb_{ads\text{-}FeOx}$ (Fig. 4B, Table 1). Fit results indicate the Pb hotspots in surficial tailings are consistent with anglesite while those in the subsurface tailings are more consistent with plumbojarosite. Although XRF map intensities are only semi-quantitative, ternary element plots indicate strong spatial correlations between Pb, Fe, and S (Fig. 4C), and that significant differences exist between the local Pb-Fe-S stoichiometries of surface and subsurface tailings. Surficial tailings have a population of Pb-Fe correlated points that are not associated with significant S (bottom right of triangles) consistent with the presence of $Pb_{ads\text{-}FeOx}$-like species.

4. DISCUSSION

4.1 Lead accumulation in small particle size fractions of surficial tailings

A striking observation contained within Fig. 1 is the 2- to 3-fold enrichment of Pb in the clay fraction that occurs across all tailings, regardless of collection depth or pH (Fig. 1B). The fact that preferential concentration of Pb in the clay-sized fraction is then compounded by an enrichment of clay-sized particles in the surficial tailings closest to the atmosphere interface (e.g., $T^{S}_{5.4}$, Fig. 1A) suggests that such colloidal particles represent an important potential vector for airborne contamination. The precise human and ecosystem health implications of Pb accumulation in fine particles at the tailings pile surface depend, however, not only on the total contaminant concentration, but also on its lability and speciation. These latter characteristics of the Pb contamination were examined using sequential extraction and X-ray absorption spectroscopy approaches, respectively.

4.2 Lead lability in Klondyke tailings

The cumulative mass of Pb extracted in the water, AA and AAO SE steps, which provides a quantitative measure of the *labile* Pb pool, is a significantly larger proportion of total Pb in surficial relative to subsurface tailings (Fig. 1C). Mine tailings Pb solubilized by H_2O and AA extractions is also soluble in stomach acid, and Pb associated with ferrihydrite has been shown to be 53–88% solubilized during the gastric portion of *in vitro* extraction.[3, 36] Hence, accumulation of this bioavailable Pb pool at the tailings-atmosphere interface may constitute a health hazard.

The lead removed in subsequent sequential extraction steps is considered less bioaccessible, but nonetheless represents a quantitative assessment that complements the XAS-based

speciation analyses discussed below. We previously reported that lead oxalate forms as a product of mineral dissolution during AAO 80 °C extraction of Klondyke tailings and that this neoformed oxalate solid is subsequently dissolved oxidatively in the H_2O_2 step.[17] Therefore, since the AAO extraction targets iron (oxyhydr)oxide and poorly crystalline jarosites known to be prevalent in these tailings, we interpret the small fraction of AAO-extractable Pb (Fig. 1C) as resulting from supersaturation and precipitation of Pb oxalate solids. Lead associated with poorly-crystalline jarosites and Fe (oxyhydr)oxides are thus accounted for in the H_2O_2 oxidation step. In addition, jarosites become increasingly crystalline with decreasing tailings pH in the field site; they persist in the most acidic ($T^D_{2.6}$) sample until the acid extraction step is complete.[17] Therefore, we interpret the release to solution during the "Acid" step for $T^D_{2.6}$ (Fig. 2) to be strong acid-induced dissolution of crystalline Pb-bearing jarosites.[17] These observations highlight the need for complementary techniques to verify the identity of contaminant molecular species contributing to analyte release during operational chemical extractions.[16, 17, 46]

4.3 Lead molecular speciation varies with collection depth

We postulated that low initial EXAFS LCF fit totals (not shown) for the tailings resulted from an underestimation of plumbojarosite because of greater variance in Pb-O bond length and higher elemental substitutions in Klondyke tailings jarosite (formed in semi-arid, near-surface weathering conditions) relative to the reference jarosite employed in the initial fits. We hypothesized that these influences could result in a decrease in the amplitude of sample EXAFS oscillations relative to the reference.[47] To test this hypothesis, a shell-by shell model was developed for a disordered plumbojarosite. LCF fits of $T^D_{2.6}$ are consistent with sequential extraction (Fig. 1C) and X-ray diffraction results[17] for $T^D_{2.6}$; Pb speciation is dominantly plumbojarosite. Three single scattering paths, developed from the crystal structure of plumbojarosite, at 2.69, 2.95, and 3.55 Å were used to fit the first two shells of the plumbojarosite reference and tailing $T^D_{2.6}$ (Fig. 3 and Table 2). Fits indicating bond distances consistent with plumbojarosite were obtained for both spectra, but a significantly higher Debye-Waller factor was obtained for $T^D_{2.6}$ than for the plumbojarosite reference, indicating a larger distribution of Pb-O distances in $T^D_{2.6}$. Greater structural disorder in the tailings plumbojarosite species (used to compute the LCF results shown in Table 1) could arise from atom substitution, defects, and small particle size, since thermal atomic motion was minimized by collecting spectra at cryogenic temperatures.[47, 48]

Overall, bulk XAS results indicate that a disordered plumbojarosite is the principle Pb-bearing phase in the Klondyke tailings, but that a significant mass fraction of anglesite is also present (Table 1). Anglesite dissolution is likely the principal contributor to labile Pb release in the AA-step of the sequential extraction and this phase, therefore, represents a bioaccessible mineral Pb species that evidently accumulates in the surficial tailings. Anglesite enrichment at the tailings surface is also consistent with the formation of efflorescent salt that was observed to precipitate on the surface of tailings subjected to irrigation during a greenhouse phytostabilization experiment (Fig.2).

X-ray fluorescence maps revealed elemental correlations and locate zones of high Pb concentration (i.e., "hotspots") for micro-focused XAS investigation (Fig. 4). The micro-focused results corroborate bulk XAS (Table 1) and SE (Fig. 1C) data by identifying hotspots consistent with anglesite in surficial tailings, and with plumbojarosite in subsurface tailings. However, they also identify the presence of Pb in a coordination environment represented by $Pb_{ads\text{-}FeOx}$ species. Relatively low mass fraction of the Pb in sorbed species represented by $Pb_{ads\text{-}FeOx}$ evidently precluded their inclusion in the bulk LCFs (Table 1), but observation of Pb enrichment co-located with Fe oxide is consistent with the known high affinity of Fe oxide surfaces for the Pb^{2+} ion.[49, 50] Since including the spectrum of $Pb_{ads\text{-}FeOx}$ did not significantly improve fits to bulk XAS data, it is probably not a dominant

lead-bearing phase in these tailings. However, it should be noted that the sensitivity of XAS to sorbed species is limited by low backscattering amplitude, and this may have also contributed to the fact that such a species was not required for the bulk fits. The identification of localized "hotspots" of $Pb_{ads\text{-}FeOx}$ particles in the surficial tailings is significant in that these particles can present Pb in a labile (e.g., adsorbed and hence exchangeable) bonding environment that could contribute bioavailable Pb in biofluids. Detection of such species only in micro-focused mode demonstrates the importance of confirming bulk measurements with grain-scale investigations.

4.4 Health Implications of Pb species distributions

Results of this study indicate that Pb contamination at a sulfide-ore mine tailings site subjected to weathering under semi-arid conditions was preferentially concentrated in the < 2 μm particle size fraction that is susceptible to aeolian off site transport. Prior work reported 15–41% dissolution of Pb in dust sized particles derived from mine tailings in simulated lung fluid extractions.[21] Particles of this size, when inhaled or ingested, travel deep into lung or gastrointestinal tissue, where they may dissolve, releasing particle-associated contaminants into lung fluid or stomach acid, with dissolution kinetics depending on the specifics of contaminant and particle speciation. In Klondyke tailings, Pb speciation is dominated by plumbojarosite. However, fits to XAS data suggest that up to 17% of Pb mass in the surficial tailings is represented by anglesite, a relatively soluble Pb mineral phase. Anglesite is considered a bioavailable form of lead that is soluble in stomach acid. Because anglesite, like Pb overall, is enriched in the clay size fraction, which in turn is enriched in the surficial tailings, it could be readily transported offsite to locations where it may be either inhaled, ingested, or deposited as dust. These observations point not only to the necessity of remediating exposed tailings piles (e.g., via capping or phytostabilization) against wind and water erosion when feasible to do so, but also to the need for careful characterization of the mobile surface depths of metal contaminated sites in order to better assess risk to surrounding communities. Particle size measurements can be integrated with multi-faceted assessment of metal speciation and lability to better characterize exposure risks deriving from mine waste systems.

Supplementary Material

Refer to Web version on PubMed Central for supplementary material.

Acknowledgments

This research was supported by Grants 2 P42 ES04940-11 and 1 R01ES017079-01 from the National Institute of Environmental Health Sciences, Superfund Research Program, NIH. Portions of this research were carried out at Stanford Synchrotron Radiation Laboratory, a National User Facility operated by Stanford University on behalf of the U.S. Department of Energy, Office of Basic Energy Sciences. The SSRL Structural Molecular Biology Program is supported by the Department of Energy, Office of Biological and Environmental Research, and by the National Institutes of Health, National Center for Research Resources, Biomedical Technology Program. Portions of this research were carried out at Advanced Photon Source, Argonne National Laboratory, Geo-Soil-Enviro-CARS, Beamline 13-BM-D, which is supported by the U. S. Department of Energy, Office of Science, Office of Basic Energy Sciences, under Contract No. DE-AC02-06CH11357. We are grateful to Matt Newville, Robert Downs, Kira Runtzel, Nicolas Perdrial, Scott White, and Mary Kay Amistadi for assistance with sample collection and analyses.

8. REFERENCES

1. Breshears DD, Whicker JJ, Johansen MP, Pinder JE. Wind and water erosion and transport in semi-arid shrubland, grassland and forest ecosystems: Quantifying dominance of horizontal wind-driven transport. Earth Surf. Processes Landforms. 2003; 28(11):1189–1209.

2. Larney FJ, Cessna AJ, Bullock MS. Herbicide transport on wind-eroded sediment. J. Environ. Qual. 1999; 28(5):1412–1421.
3. Schaider LA, Senn DB, Brabander DJ, McCarthy KD, Shine JP. Characterization of zinc, lead, and cadmium in mine waste: Implications for transport, exposure, and bioavailability. Environ. Sci. Technol. 2007; 41(11):4164–4171. [PubMed: 17612206]
4. Plumlee, GS.; Ziegler, TL.; Lollar, BS. The medical geochemistry of dusts, soils, and other earth materials. In: Holland, HD.; Turekian, KK., editors. Environmental geochemistry. Vol. Vol. 9. Elsevier; Amsterdam: 2005. p. 263-310.
5. Derry LA, Chadwick OA. Contributions from earth's atmosphere to soil. Elem. 2007; 3(5):333–338.
6. Pingitore NE Jr. Clague JW, Amaya MA, Maciejewska B, Reynoso JJ. Urban airborne lead: X-ray absorption spectroscopy establishes soil as dominant source. Plos One. 2009; 4(4):e5019–e5019. [PubMed: 19340295]
7. Benin AL, Sargent JD, Dalton M, Roda S. High concentrations of heavy metals in neighborhoods near ore smelters in northern mexico. Environ. Health Pers. 1999; 107(4):279–284.
8. CDC Blood lead levels-- united states, 1999–2002. 2005; 54(29):513–516.
9. Canfield RL, Henderson CR, Cory-Slechta DA, Cox C, Jusko TA, Lanphear BP. Intellectual impairment in children with blood lead concentrations below 10 mu g per deciliter. N. Engl. J. Med. 2003; 348(16):1517–1526. [PubMed: 12700371]
10. Gulson BL, Davis JJ, Mizon KJ, Korsch MJ, Law AJ, Howarth D. Lead bioavailability in the environment of children - blood lead levels in children can be elevated in a mining community. Arch. Environ. Health. 1994; 49(5):326–331. [PubMed: 7944562]
11. Casteel SW, Weis CP, Henningsen GM, Brattin WJ. Estimation of relative bioavailability of lead in soil and soil-like materials using young swine. Environ. Health Pers. 2006; 114(8):1162–1171.
12. Davis A, Ruby MV, Bergstrom PD. Factors controlling lead bioavailability in the butte mining district, montana, USA. Environ. Geochem. Health. 1994; 16(3–4):147–157.
13. Ruby MV, Davis A, Kempton JH, Drexler JW, Bergstrom PD. Lead bioavailability- dissolution kinetics under simulated gastric conditions. Environ. Sci. Technol. 1992; 26(6):1242–1248.
14. Hall GEM, Vaive JE, Beer R, Hoashi M. Selective leaches revisited, with emphasis on the amorphous fe oxyhydroxide phase extraction. J. Geochem. Explor. 1996; 56(1):59–78.
15. McCarty DK, Moore JN, Marcus WA. Mineralogy and trace element association in an acid mine drainage iron oxide precipitate; comparison of selective extractions. 1998; 13(2):165–176.
16. Calmano W, Mangold S, Welter E. An xafs investigation of the artefacts caused by sequential extraction analyses of pb-contaminated soils. Fresenius J. Anal. Chem. 2001; 371(6):823–830. [PubMed: 11768472]
17. Hayes SM, White SA, Thompson TL, Maier RM, Chorover J. Changes in lead and zinc lability during weathering-induced acidification of desert mine tailings: Coupling chemical and micro-scale analyses. Appl. Geochem. 2009; 24(12):2234. [PubMed: 20161492]
18. Marschner B, Welge P, Hack A, Wittsiepe J, Wilhelm M. Comparison of soil pb in vitro bioaccessibility and in vivo bioavailability with pb pools from a sequential soil extraction. 2006; 40(8):2812–2818.
19. Juhasz AL, Weber J, Smith E. Impact of soil particle size and bioaccessibility on children and adult lead exposure in pen-urban contaminated soils. 2011; 186(2–3):1870–1879.
20. Schroder JL, Basta NT, Casteel SW, Evans TJ, Payton ME, Si J. Validation of the in vitro gastrointestinal (ivg) method to estimate relative bioavailable lead in contaminated soils. 2004; 33(2):513–521.
21. Wragg J, Klinck B. The bioaccessibility of lead from welsh mine waste using a respiratory uptake test. 2007; 42(9):1223–1231.
22. Bruce S, Noller B, Matanitobua V, Ng J. In vitro physiologically based extraction test (pbet) and bioaccessibility of arsenic and lead from various mine waste materials. 2007; 70(19):1700–1711.
23. Smith E, Kempson IM, Juhasz AL, Weber J, Rofe A, Gancarz D, Naidu R, McLaren RG, Graefe M. In vivo-in vitro and xanes spectroscopy assessments of lead bioavailability in contaminated periurban solis. 2011; 45(14):6145–6152.

24. Smith E, Weber J, Naidu R, McLaren RG, Juhasz AL. Assessment of lead bioaccessibility in peri-urban contaminated soils. 2011; 186(1):300–305.
25. Davis A, Drexler JW, Ruby MV, Nicholson A. Micromineralogy of mine wastes in relation to lead bioavailability, butte, montana. Environ. Sci. Technol. 1993; 27(7):1415–1425.
26. Dold B, Fontbote L. Element cycling and secondary mineralogy in porphyry copper tailings as a function of climate, primary mineralogy, and mineral processing. J. Geochem. Explor. 2001; 74(1–3):3–55.
27. Hudson-Edwards KA, Schell C, Macklin MG. Mineralogy and geochemistry of alluvium contaminated by metal mining in the rio tinto area, southwest spain. Appl. Geochem. 1999; 14(8): 1015–1030.
28. Hudson-Edwards KA, Macklin MG, Curtis CD, Vaughan DJ. Processes of formation and distribution of pb-, zn-, cd-, and cu-bearing minerals in the tyne basin, northeast england: Implications for metal-contaminated river systems. Environ. Sci. Technol. 1996; 30(1):72–80.
29. Ostergren JD, Brown GE, Parks GA, Tingle TN. Quantitative speciation of lead in selected mine tailings from leadville, co. Environ. Sci. Technol. 1999; 33(10):1627–1636.
30. Ramos Arroyo YR, Siebe C. Weathering of sulphide minerals and trace element speciation in tailings of various ages in the guanajuato mining district, mexico. Catena. 2007; 71(3):497–506.
31. Romero FM, Armienta MA, Gonzalez-Hernandez G. Solid-phase control on the mobility of potentially toxic elements in an abandoned lead/zinc mine tailings impoundment, taxco, mexico. Appl. Geochem. 2007; 22(1):109–127.
32. Meza-Figueroa D, Maier RM, de la O-Villanueva M, Gómez-Alvarez A, Moreno-Zazueta A, Rivera J, Campillo A, Grandlic CJ, Anaya R, Palafox-Reyes J. The impact of unconfined mine tailings in residential areas from a mining town in a semi-arid environment: Nacozari, sonora, mexico. Chemosphere. 2009; 77(1):140–147. [PubMed: 19500816]
33. Brown GE, Foster AL, Ostergren JD. Mineral surfaces and bioavailability of heavy metals: A molecular-scale perspective. Proc. Natl. Acad. Sci. U. S. A. 1999; 96(7):3388–3395. [PubMed: 10097048]
34. Morin G, Ostergren JD, Juillot F, Ildefonse P, Calas G, Brown GE. Xafs determination of the chemical form of lead in smelter-contaminated soils and mine tailings: Importance of adsorption processes. Am. Mineral. 1999; 84(3):420–434.
35. O'Day PA, Carroll SA, Waychunas GA. Rock-water interactions controlling zinc, cadmium, and lead concentrations in surface waters and sediments, us tri-state mining district. 1. Molecular identification using x-ray absorption spectroscopy. Environ. Sci. Technol. 1998; 32(7):943–955.
36. Beak DG, Basta NT, Scheckel KG, Traina SJ. Bioaccessibility of lead sequestered to corundum and ferrihydrite in a simulated gastrointestinal system. 2006; 35(6):2075–2083.
37. Beak DG, Basta NT, Scheckel KG, Traina SJ. Linking solid phase speciation of pb sequestered to birnessite to oral pb bioaccessibility: Implications for soil remediation. 2008; 42(3):779–785.
38. Hayes SM, O'Day PA, Webb SM, Maier RM, Chorover J. Spectroscopic investigation of zinc speciation changes with ph in arid mine tailings in aravaipa canyon, arizona. Environ. Sci. Technol. 2011; 45:7168–7172.
39. Arai Y, Lanzirotti A, Sutton S, Davis JA, Sparks DL. Arsenic speciation and reactivity in poultry litter. Env. Sci. Technol. 2003; 37(18):4083–4090. [PubMed: 14524439]
40. Dold B. Speciation of the most soluble phases in a sequential extraction procedure adapted for geochemical studies of copper sulfide mine waste. J. Geochem. Explor. 2003; 80(1):55–68.
41. Burt R. Soil physical and fabric-related analyses. *Soil survey laboratory methods manual*; Soil Survey Investigations Report: National Resources Conservation Service 2004. Vol. 42:34–43. [PubMed: 10832934]
42. Webb SM. Sixpack: A graphical user interface for xas analysis using ifeffit. Phys. Scr. 2005; T115:1011–1014.
43. Newville M, Livins P, Yacoby Y, Rehr JJ, Stern EA. Near-edge x-ray-absorption fine-structure of pb - a comparison of theory and experiment. Phys. Rev. B. 1993; 47(21):14126–14131.
44. Webb, SM. Sam's microprobe analysis tool kit. http://www-ssrl.slac.stanford.edu/~swebb/smak.htm

45. Szymanski JT. The crystal-structure of plumbojarosite pb[fe$_3$(so$_4$)$_2$(oh)$_6$]$_2$. Can. Mineral. 1985; 23:659–668.

46. Scheinost AC, Kretzschmar R, Pfister S. Combining selective sequential extractions, x-ray absorption spectroscopy, and principal component analysis for quantitative zinc speciation in soil. Environ. Sci. Technol. 2002; 36(23):5021–5028. [PubMed: 12523415]

47. Eisenberger P, Brown GS. Study of disordered systems by exafs - limitations. Solid State Commun. 1979; 29(6):481–484.

48. Brown GE, Calas G, Waychunas GA, Petiau J. X-ray absorption-spectroscopy and its applications in mineralogy and geochemistry. Rev. Mineral. 1988; 18:431–512.

49. McKenzie RM. Adsorption of lead and other heavy-metals on oxides of manganese and iron. Aust. J. Soil Res. 1980; 18(1):61–73.

50. Webster JG, Swedlund PJ, Webster KS. Trace metal adsorption onto an acid mine drainage iron(iii) oxy hydroxy sulfate. Environ. Sci. Technol. 1998; 32(10):1361–1368.

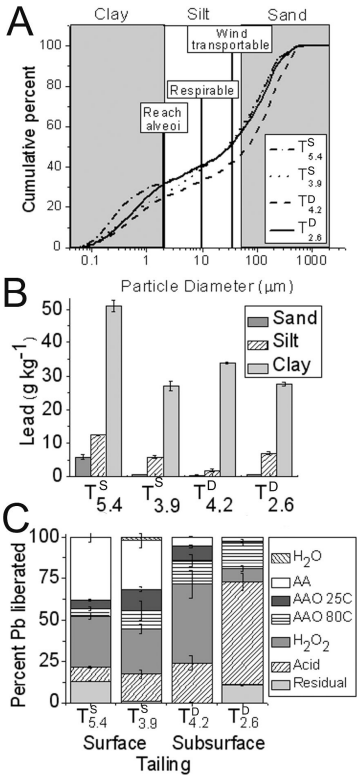

Figure 1. Particle size distribution by mass, metal content by size fraction, and Pb sequential extraction

A) Particle size analysis of tailings, B) Lead content of tailings by size fraction (sand >2 mm, silt >20 um, clay 2 um), C) Sequential extraction of lead from whole tailings (modified from Hayes et al., 2009). Sequential extraction steps: water (H_2O), ammonium acetate (AA), ammonium oxalate at 25°C (AAO 25C), ammonium oxalate at 80°C (AAO 80C), hydrogen peroxide (H_2O_2), nitric and hydrochloric acids (Acid), and residual.

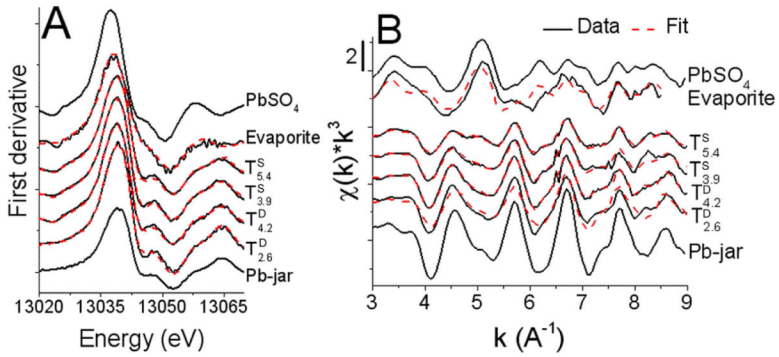

Figure 2. Linear combination fits of tailings using plumbojarosite (Pb-jar) and anglesite ($PbSO_4$)
A) first-derivative XANES (arbitrary units), B) normalized EXAFS. Fits shown by dashed line and results are presented in Table 1.

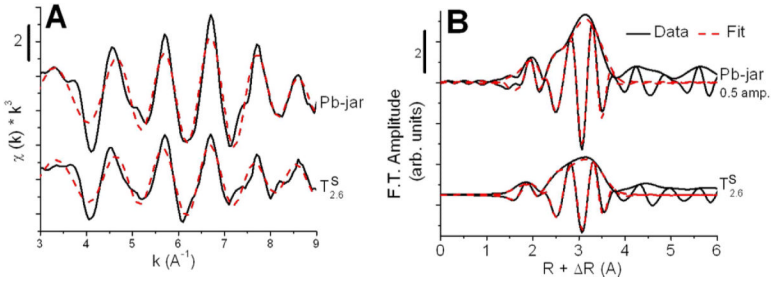

Figure 3. Shell-by-shell EXAFS fits of plumbojarosite reference and $T^{D}_{2.6}$

A) fit shown in k-space, B) fit magnitude and imaginary portion of Fourier transform. Fit parameters are tabulated in Table 2.

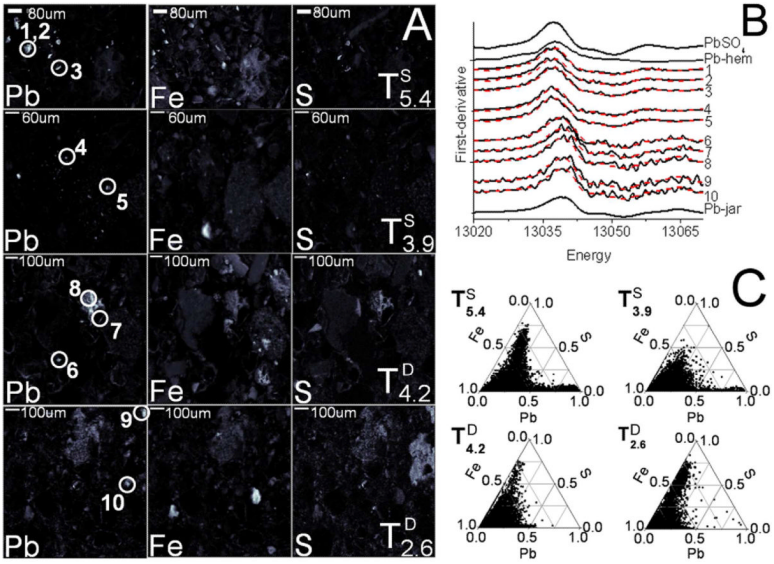

Figure 4. Grain scale phase determinations

A) XRF maps with points of μ-XAS analysis indicated, B) micro-focused X-ray absorption derivative spectra (see Table 1 for fit details), C) correlation plots.

Table 1

Linear combination fit results of bulk tailings X-ray absorption spectra.

		Sample		Pb-jar	$PbSO_4$	$Pt_{ads\text{-}FeOx}$	Sum	χ^2	Red. χ^2
(A) Derivative [a]	**Evaporite** [c]			7	93		100	0.0086	6.2E-6
	Surface	$T^S_{5.4}$ [c]		80	16		96	0.0033	3.3E-6
		$T^S_{3.9}$ [c]		83	17		99	0.0030	3.1E-6
	Subsurface	$T^D_{4.2}$ [c]		82	15		98	0.0033	3.3E-6
		$T^D_{2.6}$		100	0		100	0.0051	5.1E-6
(B) EXAFS [b]	**Evaporite** [c]			21	92		113	39.7	0.25
	Surface	$T^S_{5.4}$ [c]		58	17		83	1.75	0.015
		$T^S_{5.4}$ [c]		72	6		78	8.07	0.07
	Subsurface	$T^D_{4.2}$ [c]		93	0		93	3.35	0.02
		$T^D_{2.6}$		62	0		62	15	0.12
(C) μ-XANES derivative [a]	**Surface**	$T^S_{5.4}$	1	0	75	18	93	0.03	
			2	0	76	16	92	0.05	
			3	0	79	18	97	0.02	
		$T^S_{3.9}$	4	0	78	16	94	0.03	
			5	0	82	15	97	0.02	
	Subsurface	$T^D_{4.2}$	6	62	39	0	101	0.05	
			7	95	0	0	95	0.12	
			8	96	0	0	96	0.10	
		$T^D_{2.6}$	9	98	0	0	98	0.15	
			10	96	0	0	96	0.10	

A) first-derivative XANES spectra, B) EXAFS, and C) first derivative micro-XANES spectra collected 3 at indicated points in the XRF maps (Fig. 5b). Fits indicate percent of each component (Plumbojarosite [Pb-jar], anglesite [$PbSO_4$], and iron sorbed to iron oxides using a hematite model [$Pb_{ads\text{-}FeOx}$]) used to fit each spectrum. Spectra and fits are plotted in Figs. 2 and 4.

[a] First-derivative XANES fitting range was 13020 to 13070 eV.

[b] EXAFS fits were performed over the k-range 3–9 $Å^{-1}$.

[c] Fit using $T^D_{2.6}$ as the plumbojarosite reference.

Table 2

Shell-by-shell EXAFS fit summary for plumbojarosite reference and $T^{D}_{2.6}$, shown in Figure 3.

	E_0 (eV)	path	N	Distance (Å)	σ^2 (Å^2)	Red χ^2
Pb-jarosite structure [a]		Pb-O Pb-O Pb-Fe	6 6 6	2.69 2.95 3.55		
Pb-jar	4.1 (2.1)	Pb-O Pb-O Pb-Fe	6[b] 6[b] 6[b]	2.67 (3) 2.94 (3) 3.57 (2)	0.014 (3) 0.009 (2) 0.0088 (8)	429
$T^{D}_{2.6}$	4.8 (2.2)	Pb-O Pb-O Pb-Fe	6[b] 6[b] 6[b]	2.67 (4) 2.95 (4) 3.60 (2)	0.023 (4) 0.014 (3) 0.014(1)	138

Fitted parameters included: E_0, energy shift; path, single-scattering absorber-backscatterer (A–B) pair; N, path degeneracy; distance, A–B distance; σ^2, Debye-Waller factor (mean-square bond displacement); reduced χ^2, statistical goodness-of-fit. Error estimates of fitted parameters are shown in parenthesis.

[a] Szymanski, 1985.

[b] Fixed during fitting.